Applied Clay Science 205 (2021) 106036

Contents lists available at ScienceDirect

Applied Clay Science

journal homepage: www.elsevier.com/locate/clay

Research Paper

The alteration of Miraflores Basalt (Panama): Mineralogical and textural evolution

Emilia García-Romero [a,b,*], Mercedes Suárez [c]

[a] Department of Mineralogy and Petrology, Complutense University of Madrid, 28040 Madrid, Spain
[b] Geosciences Institute (IGEO), Spanish Research Council and Complutense University (CSIC-UCM), 28040 Madrid, Spain
[c] Department of Geology, University of Salamanca, 37008 Salamanca, Spain

ARTICLE INFO

Keywords:
Palagonite
Iddingsite
Bentonite
Basalt alteration
Miraflores Basalt
Panama Channel

ABSTRACT

Samples of The Miraflores Basalt sub-volcanic rocks (Miocene Late Basalt Formation) collected from different quarries on the Isthmus of Panama and several samples collected from the excavation of the third set of locks in the New Panama Channel were characterised in this study. All rocks studied had similar petrological and mineralogical characteristics; however, the samples had substantially different degrees of alteration, which varied in the NW–SE direction. The most altered areas were located at the SE (Sosa Hill Quarry), next to the Pacific Ocean, while the Cerro Escobar rocks, located further inland, showed only slight alteration. The rocks from the excavation and from the Cocolí and Aguadulce Hills area, located in the middle of the study region, exhibit features consistent with intermediate alteration between the two aforementioned extreme cases. Images and data from different alteration stages were obtained using optical microscopy, electron microprobe (EMP), and scanning electron microscopy (SEM). The earliest stage of alteration was characterised by the presence of iddingsite, which was almost the only product of alteration. As the alteration progressed, the generalisation of smectites throughout the rock was characteristic. The glass disappeared and transformed to palagonite, and the plagioclase and pyroxene crystals became altered both at the edges and inside the crystals. The crystals also showed numerous nanofractures, which were mainly perpendicular to the longer faces and that were filled by smectite. In the most advanced alteration state, all crystals and glass were deeply affected. Crystals were deeply transformed into smectite, and the porosity of the rock increased in a process that conserved the volume. Smectite appeared as the end-alteration product both from the major minerals (olivine, plagioclase, pyroxenes), as well as from the glass.

1. Introduction

The alteration of basaltic rocks has been studied extensively (Craigh and Loughnan, 1964; Böhlke et al., 1980; Eggleton et al., 1987; Smith et al., 1987; Fookes et al., 1988; Bhattacharyya et al., 1992; Thanachit et al., 2006; Vingiani et al., 2010; Churchman and Lowe, 2012; Fontaine et al., 2020; among others). Alteration includes the alteration of volcanic glass but also the alteration of the other minerals that compose the rock and occurs until these minerals are completely or almost completely transformed into clay minerals. Nesbitt and Wilson (1992) affirmed that basaltic weathering profiles are not greatly affected by primary mineralogy or by bulk composition of the parent basalt, probably because major silicate phases are weathered at grossly similar rates. The admitted rate of weathering of individual minerals is consistent with the well-known susceptibility series: glass > olivine > pyroxene > amphibole > plagioclase > K-feldspar> opaque minerals (Craigh and Loughnan, 1964; Colman, 1982; Eggleton et al., 1987). Although Nesbitt and Wilson (1992) affirmed that "local equilibrium, and kinetic considerations indicate that there is no fixed order of mineral susceptibility to weathering and no fixed leaching order of elements from basalts. Only after classification of a basalt according to bulk composition and model proportions can generalizations be made in these regards". Weathering occurs in successive continuous stages of increasing intensity as the alteration progresses. This requires hydration (taking up water or combining with water) and a change in the chemical composition; the textures of the original volcanic rock in the early and intermediate stages of alteration are preserved. In open microsystems transfers of elements occur by slow diffusion along the network of inter-mineral micropores

* Corresponding author at: Department of Mineralogy and Petrology, Complutense University of Madrid, 28040 Madrid, Spain.
E-mail addresses: mromero@ucm.es (E. García-Romero), a87578@usal.es, msuarez@usal.es (M. Suárez).

https://doi.org/10.1016/j.clay.2021.106036
Received 20 January 2021; Received in revised form 17 February 2021; Accepted 19 February 2021
Available online 14 March 2021

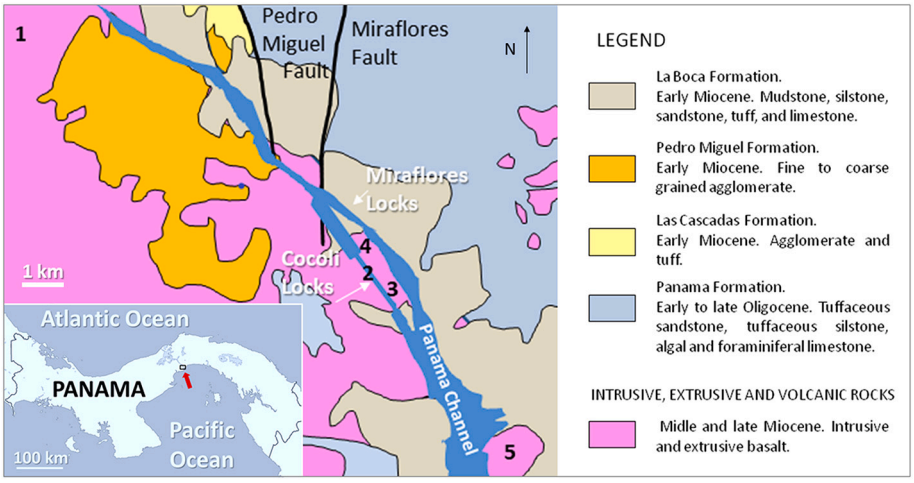

Fig. 1. Geological scheme and location of samples. 1) Cerro Escobar, 2) Excavation area. 3) Aguadulce Hill quarry, 4) Cocolí Hill quarry, 5) Sosa Hill quarry. Modified from Stewart et al. (1980).

and cracks developed inside the rock acted as direct connections between microsystems (Vingiani et al., 2010). The mobility of elements during weathering is the usual: Na + K > Ca > Mg > Si > Fe ≥ Mn ≥ Ti ≥ Al (Stefansson and Gislason, 2001). During the basalt weathering, a variety of secondary phases commonly form, including allophane, iron oxide-hydroxide, and clay minerals (kaolinite, halloysite and different composition smectites, mainly Fe-smectites) (Colman, 1982; Eggleton et al., 1987; Stefansson and Gislason, 2001; Chadwick et al., 2003; Rasmussen et al., 2010; Vingiani et al., 2010, among others). Climate controls mineral neogenesis. Weathering and mineralogical transformations developments are limited by water availability and temperature. Yesavage et al. (2015) studied experimentally the weathering of basalt and highlighted the importance of wetting/drying, thus the cyclic adsorption of water onto basaltic rocks may result in high physical spalling rates that in turn promote chemical leaching.

Under hydrothermal alteration, the composition and temperature of the fluids influence the final composition of the smectite, as do under weathering other factors, such as the climate, topography, geomorphology, and time. Giorgetti et al. (2009) studied the low-temperature hydrothermal alteration of trachybasalts found the formation of montmorillonite- and saponite-like smectite from the alteration of interstitial glass. They concluded that the reaction were strongly influenced by the glass chemistry composition and that reaction style and reaction progress were controlled by kinetic factors such as the mode of fluid transport triggering alteration in the low-temperature hydrothermal environment. In comparison to the volcanic glass, the crystalline phases were less prone to hydrothermal alteration with the alteration susceptibility decreasing from clinopyroxene through biotite to feldspar. Low-temperature alteration of clinopyroxene resulted in the formation of abundant saponite-like smectite with no topotactic relationship being observed between the two phases. In contrast, the conversion of biotite to smectite involved structural inheritance as the orientation of common structural blocks was maintained during alteration.

The mechanisms that enable smectite formation are variable. Smectites can be formed by dissolution–precipitation processes from pre-existing mineral phases or volcanic glass. In sedimentary deposits, smectites can form both by the transformation of pre-existing clay or non-clay minerals and by neoformation and direct precipitation from solutions or colloids. Neoformation by direct precipitation can also occur in hydrothermal media. It is sometimes difficult to differentiate between these mechanisms, which have been widely studied by numerous authors (Ugolini, 1974; Delvaux and Herbillon, 1995; Righi et al., 1999; Huertas et al., 2000; Christidis, 2001, 2006; Velde and Meunier, 2008; Christidis and Hu, 2009; Cuadros et al., 2011; Lacoviello et al., 2012; Manuella et al., 2012; García-Romero et al., 2005, 2019; Kadir et al., 2017; among others).

A mineral's susceptibility to alteration depends on its structure and chemistry (Meunier et al., 2007). Olivine and plagioclases are the first minerals formed in the discontinuous and continuous reaction series, respectively; thus, they are highly susceptible to alteration. Olivine is a highly reactive mineral that begins to transform in the early stages of volcanic rock settlement.

The alteration product of olivine is iddingsite. Iddingsite forms since the early stages of basalt formation (Delvigne et al., 1979; Eggleton, 1984; Smith et al., 1987; Banfield et al., 1990). During olivine alteration, the formation of iddingsite is generally initiated at crystal edges. Iddingsite appears to invade the crystals progressively until, in the most extensively altered samples, the original olivine is entirely transformed. Iddingsite is composed of a mixture of iron oxi-hydroxide and smectite intergrowths (Delvigne et al., 1979; Smith et al., 1987; Churchman and Lowe, 2012). Saponite, bowlingite, nontronite, vermiculite, celadonite, chlorite, serpentine, bastite, cummingtonite, hastingsite, uralite, and chlorophaeite have all been cited in the literature as alteration products of olivine or pyroxene. However, glass alters to palagonite as the first stable product of volcanic glass alteration (Stroncik and Schmincke, 2002a, 2002b). The palagonite composition varies depending on the composition of the original volcanic rock and the type and degree of alteration, according to its definition as a new mineral species (Von Waltershausen, 1845). Most researchers accept that palagonite is a heterogeneous substance composed of different clay minerals, zeolites, and/or oxides, or mixtures of these (Peacock and Fuller, 1928; Furnes, 1980, 1984; Eggleton and Keller, 1982; Jercinovic et al., 1990; Zhou et al., 1992). Feldspars, both plagioclase and K-feldspars, also progressively alter to clay minerals, depending on the climate and alteration conditions (Wilson, 2004). The dissolution–recrystallisation of feldspars leads to the formation of secondary clay minerals.

Under hydrothermal alteration, the interactions among Mg-rich fluids, glass, and primary minerals result in smectite neoformation (Środoń et al., 2019; Vingiani et al., 2010, and references therein). These smectites are mainly Fe-rich, and can be of the Fe-rich saponite type (Loughnan, 1969; Böhlke et al., 1981; Gillis and Robinson, 1990; García-Romero et al., 2005) and Fe-rich dioctahedral type (Brigatti, 1983; Decarreau et al., 1987; Köster et al., 1999; Christidis, 2006; Giorgetti et al., 2009; Rasmussen et al., 2010). The formation of dioctahedral instead of trioctahedral smectite may be related to the presence of CO_2, according Gaudin et al. (2018). Böhlke et al. (1980) argued that the formation of smectites from the alteration of basalts is related to

Table 1
Chemical composition of the samples. Major elements in % of oxides. Lower Limit detection 0.01%. A.S.: alteration state group. E: early, I: intermediate, and A: advanced.

Location	Sample	A.S.	SiO_2	Al_2O_3	Fe_2O_3	FeO	MnO	MgO	CaO	Na_2O	K_2O	TiO_2	P_2O_5	LOI
	AHQ-1		52.95	16.08	3.47	6.40	0.18	4.58	8.66	3.67	0.67	1.59	0.41	1.40
	AHQ-1B		50.96	16.27	3.78	6.70	0.18	4.22	8.63	3.47	0.67	1.60	0.39	1.23
	AHQ-2		51.85	16.67	4.01	5.50	0.16	4.55	8.57	3.48	0.65	1.41	0.37	2.17
	AHQ-2B		52.62	15.66	3.56	6.40	0.18	4.18	8.58	3.49	0.83	1.62	0.43	1.50
	AHQ-3		52.04	15.85	3.63	6.50	0.17	4.37	8.24	3.59	0.70	1.42	0.42	1.50
	AHQ-3B		51.09	15.77	4.18	6.00	0.17	4.28	8.61	3.45	0.68	1.59	0.41	1.77
	SPP-2		51.14	16.77	4.99	4.90	0.17	4.43	9.11	3.37	0.56	1.53	0.38	2.79
	SPP-1		50.29	16.78	4.71	4.80	0.16	4.80	9.77	3.42	0.46	1.38	0.34	2.56
	566-1A		52.35	15.52	4.02	5.70	0.18	4.49	8.17	3.64	0.70	1.78	0.45	2.15
	566–2		52.99	15.93	3.26	6.70	0.18	4.53	8.17	3.72	0.80	1.66	0.47	1.23
	566–3		52.24	16.20	3.45	6.70	0.18	4.42	8.46	3.69	0.78	1.65	0.47	1.28
Aguadulce	566–4		51.66	16.31	3.25	6.60	0.19	4.45	8.60	3.59	0.77	1.72	0.43	1.51
Hill	566-5A	I	52.17	15.85	3.35	6.80	0.18	4.45	8.50	3.63	0.78	1.69	0.44	1.28
Quarry	566–6		52.74	16.21	3.15	6.90	0.18	4.46	8.56	3.66	0.81	1.64	0.45	1.22
	573-1A		52.43	16.50	3.26	6.20	0.17	4.52	8.62	3.67	0.69	1.56	0.40	1.31
	573-2A		51.82	15.87	4.52	5.80	0.18	4.70	8.28	3.42	0.75	1.66	0.44	2.48
	573-3A		51.93	15.86	3.40	6.50	0.16	4.49	8.61	3.48	0.67	1.55	0.41	2.19
	573-4A		52.51	15.24	3.16	6.90	0.16	4.47	8.30	3.53	0.73	1.66	0.45	2.16
	573-5A		53.06	14.27	3.46	6.90	0.18	4.40	8.71	3.73	0.72	1.75	0.46	1.26
	573-6A		50.72	17.11	3.69	5.30	0.16	4.94	9.89	3.28	0.50	1.38	0.36	2.47
	574-1B		49.72	17.55	4.78	4.60	0.15	4.82	9.23	3.28	0.56	1.50	0.37	3.67
	574-2A		49.94	16.62	4.53	4.60	0.15	4.58	9.32	3.23	0.55	1.46	0.35	3.19
	574-3A		49.76	16.10	4.69	5.20	0.15	5.34	9.35	3.08	0.47	1.48	0.39	3.73
	574–4		51.14	16.60	3.86	5.70	0.17	4.33	9.27	3.31	0.57	1.48	0.35	2.82
	574-5B		51.40	16.78	3.79	4.60	0.15	4.39	9.93	3.21	0.49	1.27	0.29	2.95
	574-6A		48.55	17.05	5.57	5.40	0.14	5.07	9.52	3.07	0.24	1.47	0.30	3.79
C. Escobar	CES-1A		52.43	15.07	3.77	7.00	0.18	3.60	7.60	3.39	0.58	1.83	0.39	2.42
Hill	CES-2A	E	52.89	15.65	3.82	7.10	0.18	3.82	7.80	3.47	0.55	1.83	0.36	2.28
Quarry	CES-3A		52.13	15.24	2.74	7.60	0.17	3.94	7.87	3.37	0.41	1.79	0.35	3.06
	CCH-1		52.98	16.01	2.95	7.00	0.18	4.56	8.44	3.76	0.73	1.67	0.45	1.25
	CCH-2		51.92	16.40	3.63	6.50	0.17	4.45	8.73	3.56	0.67	1.59	0.42	1.24
Cocoli	CCH-3		53.64	15.81	2.92	7.00	0.18	4.42	8.15	3.83	0.81	1.69	0.44	1.20
Hill	567–1	I	49.56	17.26	4.38	5.30	0.16	4.54	9.49	3.14	0.55	1.53	0.35	3.18
Quarry	567–2		50.01	17.22	4.68	4.90	0.17	4.81	9.55	3.20	0.23	1.48	0.37	3.47
	567-3A		51.31	15.86	4.07	5.70	0.17	4.44	8.75	3.51	0.69	1.61	0.42	2.43
	567–5		49.31	17.16	4.26	5.00	0.16	5.15	9.90	3.16	0.51	1.41	0.35	3.50
	567–4		49.47	17.20	5.34	4.20	0.15	4.84	9.22	3.13	0.50	1.47	0.38	3.99
Sosa	SHQ-1A		50.84	16.18	3.34	5.40	0.16	5.11	8.85	3.21	0.46	1.28	0.22	3.37
Hill	SHQ-2A	A	51.67	16.15	3.31	5.70	0.15	5.62	9.26	3.10	0.41	1.21	0.22	3.01
Quarry	SHQ-3A		51.43	17.07	3.73	5.20	0.15	5.21	8.90	3.40	0.43	1.23	0.23	2.98
	LH-1		52.95	16.01	3.08	6.80	0.17	4.44	8.35	3.58	0.77	1.52	0.42	1.00
Excavation	LH-2	I	53.24	16.16	3.22	6.50	0.18	4.47	8.47	3.64	0.73	1.62	0.44	0.94
	TRF-1		51.81	15.88	4.26	5.70	0.18	4.62	8.98	3.34	0.61	1.52	0.40	2.22
	TRF-1b		51.03	15.96	5.06	5.10	0.17	4.71	8.93	3.36	0.56	1.52	0.35	2.95

moderate fluid circulation that avoids SiO_2 and MgO leaching.

During the construction of the third set of locks of the Panama Canal a rapid degradation of the apparent sound Miraflores Basalt resulted in the huge loss of fines during the crushing for obtaining aggregates. Such a rapid degradation of a basic igneous rocks – exposed to the weather and then utilized as a construction material – is not frequent. This forced to the constructors to modify the crushing plant and to look for a new source of raw materials for the concrete production, and it also forced to conduct an in-depth study of the Miraflores Basalts to elucidate the causes of its degradation, which was responsible for the delay in the

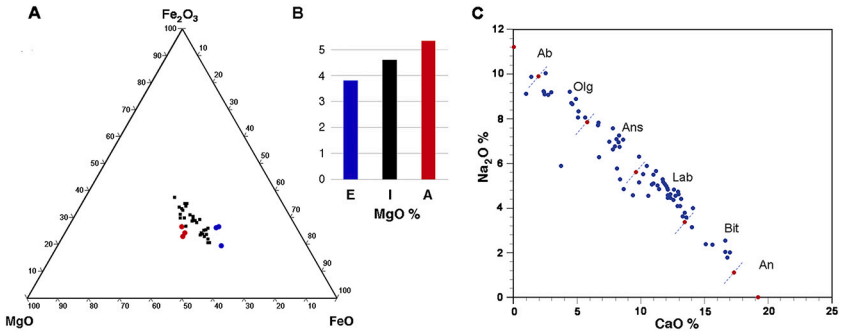

Fig. 2. A: Plot of the MgO %, Fe_2O_3%, and FeO % contents of the samples according their alteration state. Blue circle: early, black square: intermediate, and red circle: advanced. B: MgO % indicates the content of each group of samples according of their alteration stage. E: early, I: intermediate, and A: advanced. C:. Compositional variation in the plagioclases from the Miraflores Basalt. Ab: Albite, Olg: Oligoclase, Ans: Andesine, Lab: Labradorite, Bit: Bitownite, and An: Anorthite. Mineral name abbreviations after Whitney and Evans (2010).

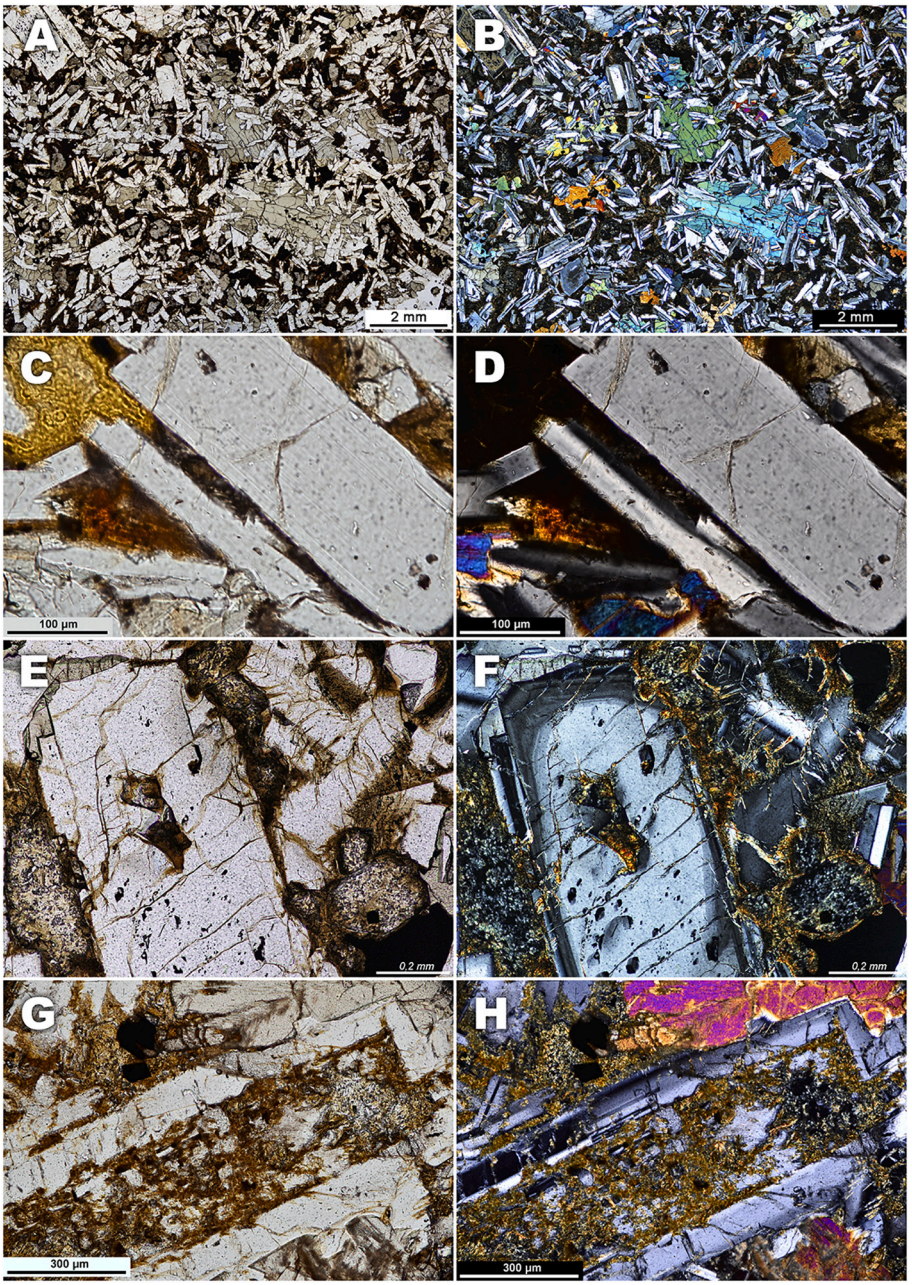

Fig. 3. Optical microscopic images of plagioclase crystals. (A, C, E, G: Transmitted light images) (B, D, F, H: Plane polarized transmitted light images). Note that the degree of alteration increases from A-B to C—D and *E*-F in the images. A-B: clean unaltered crystals. B-C: plagioclase crystals corroded at their edges and altered in their interiors. E-F: plagioclase crystals completely altered, both internally and at their edges. They resemble skeletal crystals.

construction of the third set of locks on the Panama Canal (Suárez et al., 2021). Such numerous studies resulted in a large amount of data that have allowed a much better understanding of how basalts transform.

The aim of this work is to show the mineralogical and textural changes related to the different stages of the alteration of the Miraflores Basalt. The early, intermediate, and advanced stages of the alteration of the volcanic rock are shown through images derived from optical microscopy (OM), electron microprobe (EMP) analysis, and scanning electron microscopy (SEM). The use of the electron microscopy in the study of igneous rocks is not frequent and, from our knowledge, this is the first time that the textural relationship between the primary minerals and the alteration products as the alteration progresses is shown at SEM scale.

2. Materials and methods

2.1. Materials

The samples studied are Miraflores Basalt sub-volcanic rocks (Late Miocene Basalt according to Stewart et al., 1980) from the Isthmus of Panama (Fig. 1). A wide group of samples from different areas were selected over a range of degrees of alteration. Representative samples were selected from the excavation site of the construction of the third set of locks of the Panama Canal and from quarries in three areas: Cerro Escobar, Cocolí and Aguadulce Hills, and Sosa Hill (Fig. 1).Variability in the degree of alteration was observed in the NW–SE direction. The most altered areas are located at the SE (Sosa Hill Quarry), next to the Pacific Ocean, while the rocks of Cerro Escobar are further inland and only show slight alteration. The rocks from the Cocolí and Aguadulce Hills area, located in the middle of the study region, exhibit intermediate alteration features relative to the highly and slightly altered features in the other regions. The largest number of samples studied comes from the Aguadulce Hill Quarry and Cocolí Hill quarry since they were the rock utilized in the construction of the third set of looks. The location of the samples is in Table 1.

2.2. Methods

The morphological and textural features were established using optical (OM) and scanning electron microscopy (SEM). For the OM analyses, thin sections were prepared from altered basalt samples. SEM observations were conducted at the Centro Nacional de Microscopía Electrónica (Spain) with a JEOL JSM-6330F (field emission scanning electron microscope) operated at 10 and 20 kV, wd 15 mm, and SEI, equipped with an Oxford Instruments: X-Max 80 mm^2 qualitative elemental analysis by energy dispersion spectroscopy (EDS) at 127 eV and 5.9 keV. Prior to the SEM examination, freshly fractured surfaces of representative samples were air-dried and coated with Au under a vacuum. Element maps were obtained with a Hitachi VP-SEM S-3400 N equipped with a Bruker Quantax X-Flash SDD EDS microanalyzer at 125 eV. EMP observations were conducted using a JEOL Superprobe JXA-8900 M at the Centro Nacional de Microscopía Electrónica (Spain).

Mineralogical characterisation was performed by X-ray powder diffraction of whole-rock samples powdered in a manual agate mortar. The oriented aggregates were analysed under ambient conditions, after solvation with ethylene glycol and heating the clay fraction to 550 °C. A Bruker D-8 advance XRD diffractometer with CuKα radiation and a graphite monochromator was employed for the whole rock from 2° to 65° in steps of 0.05°, with a 1 s/step counting time, and from 2° to 40° for the oriented aggregates, with steps of 0.05° at 1 s/step.

Chemical analyses of major elements were performed at Actlabs, the Activation Laboratory of Ontario (Canada). The selected analysis package was 4lithores-research, which included lithium metaborate/tetraborate fusion ICP. The fused samples were diluted and analysed using a Perlin Elmer Sciex ELAN 6000, 6100, or 9000 ICP/MS. Three blanks and five controls (three before the sample group and two afterwards) were analysed for each group of samples. The lower limit detection is 0.01%.

3. Volcanic rock

Based on their chemical composition, the Miraflores Basalts are classified as tholeiitic basalts and basaltic andesites according to Suárez et al. (2021). The chemical compositions of the samples are listed in Table 1.

Although basalts with different states of alteration were studied, no significant impact of the degree of alteration was observed for the chemical composition of the major elements; only a small variation in the MgO content was observed as the oxide content increased from the fresher to the most altered basalts (Fig. 2A-B).

In general, all the Miraflores Basalts are medium-grained and hypocrystalline because they contain some proportion of glass, although this glass may be transformed to palagonite. Texturally, these basalts are microgabbro or diabase and are composed of plagioclase, minor clinopyroxenes (ordinarily augite), and scarce orthopyroxenes and altered olivine (usually transformed to iddingsite), with abundant titanomagnetite, Fe-oxides, and variable proportions of devitrified volcanic glass, which usually contain idiomorphic apatite crystals (Fig. 3A-B). A detailed study focused on each component allows the study of the alteration evolution from the freshest to the most degraded rocks.

As is common in volcanic and subvocanic rocks, plagioclase is the most abundant constituent. Plagioclase features are similar in texture and composition in all Miraflores Basalt samples studied; the only differences are their alteration traits. According to the microprobe data shown in Fig. 2C, these samples can be classified between oligoclase and bitownite, but pure extremes of the solid solution (albite and anorthite) were not found. The crystals are randomly arranged idiomorphic to subidiomorphic from 0.5 to 2 mm (although several larger phenocrysts had lengths up to 4 mm) and they occasionally present lamellar twinning and oscillatory or concentric zoning (Fig. 3A-B). These crystals include opaque inclusions (more abundant in the phenocrysts) that are linearly arranged parallel to the longer axis and are usually responsible for crystal zonation. Plagioclase laths are frequently embedded in augite crystals in samples with sub-ophitic textures (Fig. 3 A-B). Most crystals contain fractures largely perpendicular to their longer faces, more frequently in the phenocrysts however, the number of fractures varies widely among the three studied areas, according to the alteration grade of the rocks (Fig. 3). According to Farris et al. (2017), these basalts can be differentiated from the Pedro Miguel basaltic lava flows that also outcrop in the area because their phenocrysts are mainly euhedral and are occasionally composed of aligned plagioclases, while the pyroxenes appear primarily as sub- to anhedral crystals among and around the plagioclases.

Abundant iddingsite is present in all Miraflores Basalt samples, which indicates the pre-existence of olivine. The presence of iddingsite in the Miraflores Basalts is consistent with their tholeiitic character. However, olivine in fresh rocks is often already altered by magmatic and metamorphic transformations and by deuteric or hydrothermal processes to iddingsite.

Pyroxenes (clinopyroxenes and orthopyroxenes) are minor components compared to plagioclases. The clinopyroxenes (augite) are much more abundant than orthopyroxenes (which may even be absent). They usually appear as allotriomorphic phenocrysts, which are less than 1 mm in size (Fig. 3A-B). In several instances, the clinopyroxenes are simple or lamellar zoned. Opaque minerals (Ti-magnetite) were abundant in all samples. These minerals are composed of idiomorphic to subidiomorphic crystals. They appear both in the matrix and in the crystals. In several instances, smaller altered crystals are part of the alteration mass in the matrix alongside the glass. Additionally, prismatic apatite crystals are frequent in the glass.

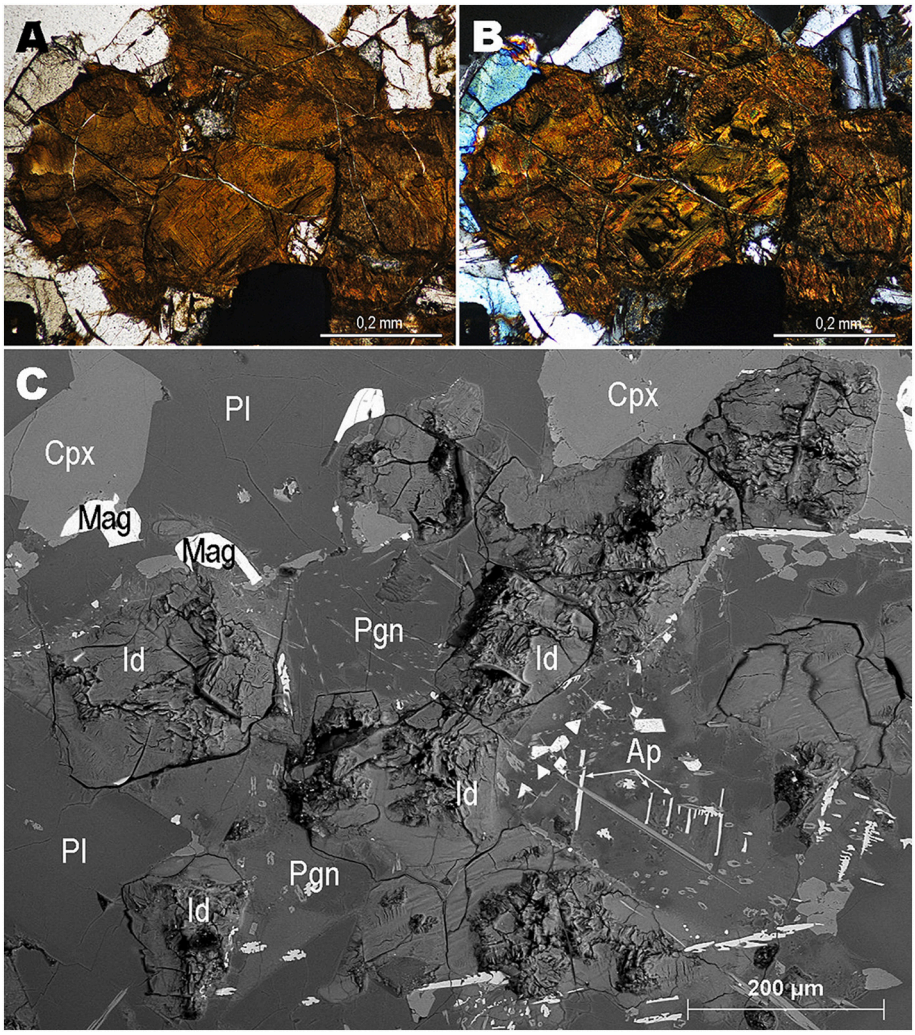

Fig. 4. Iddingsite images. A-B: Optical microscopic images of iddingsite grains included in a matrix of plagioclase and clinopyroxene crystals. A: Transmitted light image. B: Plane polarized transmitted light image. C: Backscattered electron SEM image. Ap: Apatite, Mag: Magnetite, Pl: Plagioclase, Pgn: Palagonite, Cpx: Clinopyroxene, and Id: Iddingsite. Mineral name abbreviations after Whitney and Evans (2010).

4. Early stage of alteration

The early stage of alteration of the Miraflores Basalts is characterised by the presence of iddingsite as almost the only product of alteration. The samples that exhibit this lower degree of alteration are from the Cerro Escobar quarry. In these samples, glass, feldspars and pyroxenes remain unaltered (Fig. 3C-D) and only olivine is altered. Olivine is the first mineral to alter to iddingsite in the earlier stages of volcanic rock alteration, as has been previously noted. Iddingsite, when observed with an optical microscope, appears as small orange to brown reddish-brown grains with high relief, which resembles the appearance of olivine. Generally, fibres growing inside these grains are easily seen at high magnification in both optic (Fig. 4A-B) and electronic microscopy. Fig. 4C shows a back-scattered electron image, which clearly shows the iddingsite grains included in the matrix. In addition, other primary minerals such as plagioclases and clinopyroxenes can be recognised since they show different grey tones that depend on their chemical composition in the back-scattered images. The transformation from olivine to iddingsite has been studied in detail by several authors (Eggleton, 1984; Smith et al., 1987; Banfield et al., 1990). It is generally agreed that iddingsite is composed of a mixture of smectites and Fe-oxides. The transformation process can occur in successive stages and very often begins at the moment of rock placement. The structural mechanism by which olivine transforms to smectite and the significance of the topotactic reactions were discussed by Eggleton (1984). Smith et al. (1987) also described olivine alteration to saponite and goethite, and the subsequent development of goethite. Banfield et al. (1990), state that 'observations by TEM from basalt that in thin-section shows little evidence of weathering indicate that replacement of olivine involves the formation of dissolution channels and the growth of smectite and hematite'. According to these studies, in the samples from the Cerro Escobar quarry, the olivine appears iddingsitised and is the only altered mineral, which indicates that these rocks are fresher than the others studied.

In the earlier alteration stages of the volcanic Miraflores Basalts (Cerro Escobar samples), the plagioclase and pyroxene surfaces were smooth when observed by SEM. Incipient alteration of these minerals was observed only sparingly. In these cases, the alteration began with the growth of small and sporadic smectite flakes on the crystal surfaces, as observed in the SEM images (Fig. 5A, B). In several instances, isolated flakes grew in a concentrically distributed (Fig. 5C). In this stage of incipient alteration, the presence of volcanic glass is characteristics. It is easily identified by optical microscopy and was found only in the Cerro Escobar samples. At this stage, the rock components are strongly fused; consequently, it is difficult to differentiate the minerals from the glass by SEM (Fig. 6A). The unaltered glass (Fig. 6B) cracks, and as the alteration progresses new cracks appear sporadically and radially around a point (Fig. 6C).

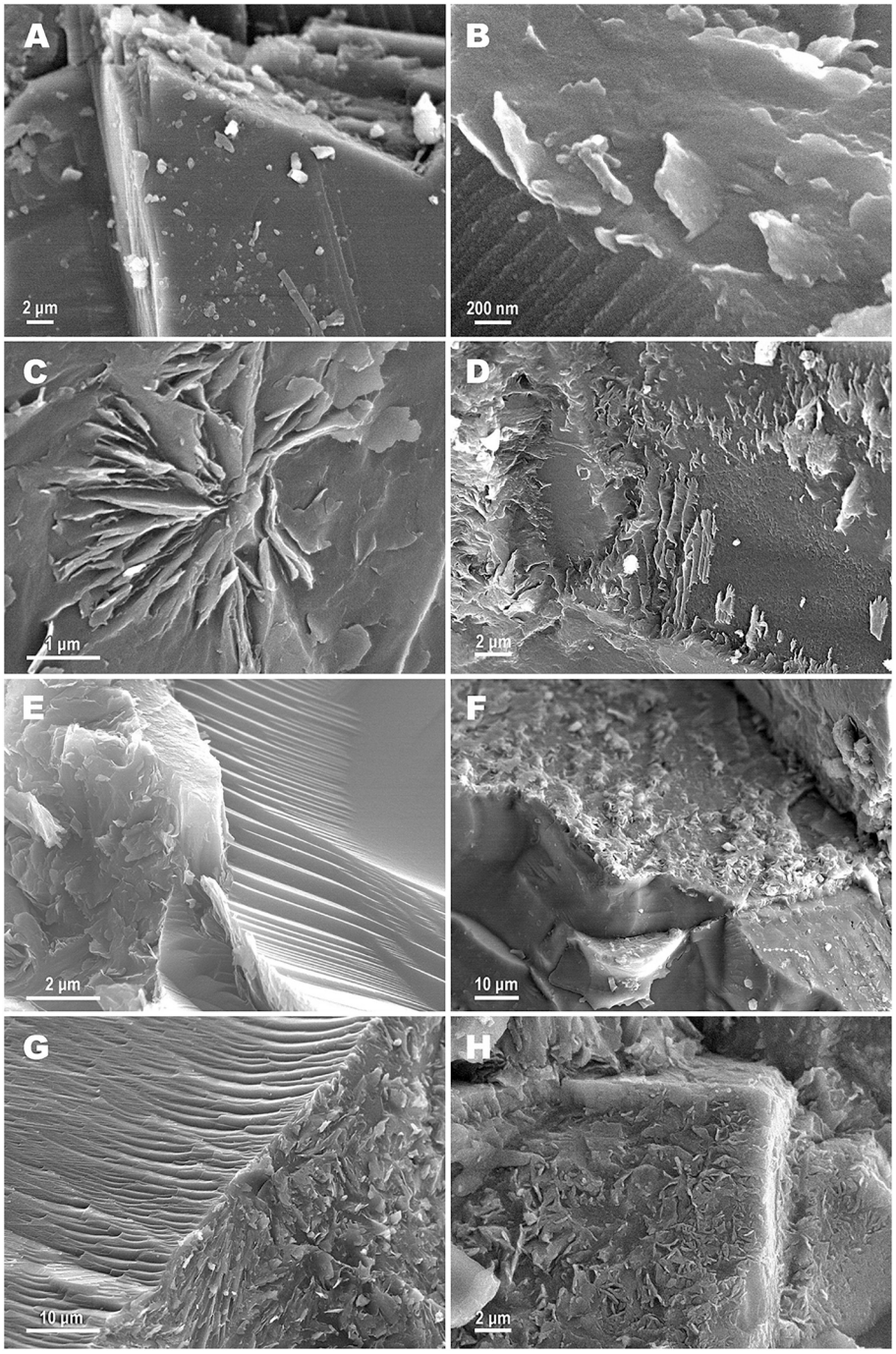

Fig. 5. Scanning electron microscopy (SEM) images. The images illustrate the evolution of plagioclase alteration. A: Unaltered plagioclase surface. B: Isolate flakes growing on the surface. C: Flakes growing in a concentrical arrangement. D: Abundant flakes growing and covering the plagioclase crystal surfaces. E: Growing flakes emerging of the crystal surface, opening popcorn-like. F: The different crystallographic faces show different alteration patterns. G and H: Plagioclase crystals completely altered.

5. Intermediate stage of alteration

In the intermediate stage of alteration of the Miraflores Basalt, the presence of smectites throughout the full rock is characteristic. The progress of alteration of affecting the rock is evident by the disappearance of glass and the alteration of the plagioclase and pyroxene crystals. Plagioclases, both phenocrysts and groundmass, independently of their size, show alteration effects, although larger crystals have higher alteration. They are altered both at the edges and insides of the crystals and show numerous nanofractures mainly perpendicular to the longer faces that are filled by smectite (Fig. 3E-F). The alteration, thus, is usually favoured by fractures, zoning, and inclusions. When observed with optical microscopy, every crystal has a brownish colour at inside and at the edges, which are corroded by the alteration.

The progress of the plagioclase alteration is also clearly illustrated by the SEM images in (Fig. 5). As the alteration advances, the flakes become more abundant, covering the surfaces of plagioclase crystals more profusely (Fig. 5D), and becoming the majority. Sometimes, growing flakes emerge from the crystal surface opening as popcorn, as shown in Fig. 5E. It is remarkable that the surfaces of the plagioclase crystals show different degrees of alteration depending on their crystallographic orientation indicating the structural control (Fig. 5F).

Abundant and contradictory literature has been devoted to the study of the alteration of alkali feldspars and plagioclases under natural and experimental conditions (see the review of Wilson, 2004 and references therein). When the parent crystals are altered both at the insides and on their surfaces, their secondary products are not always the same. In other words, a given parent mineral species does not produce the same

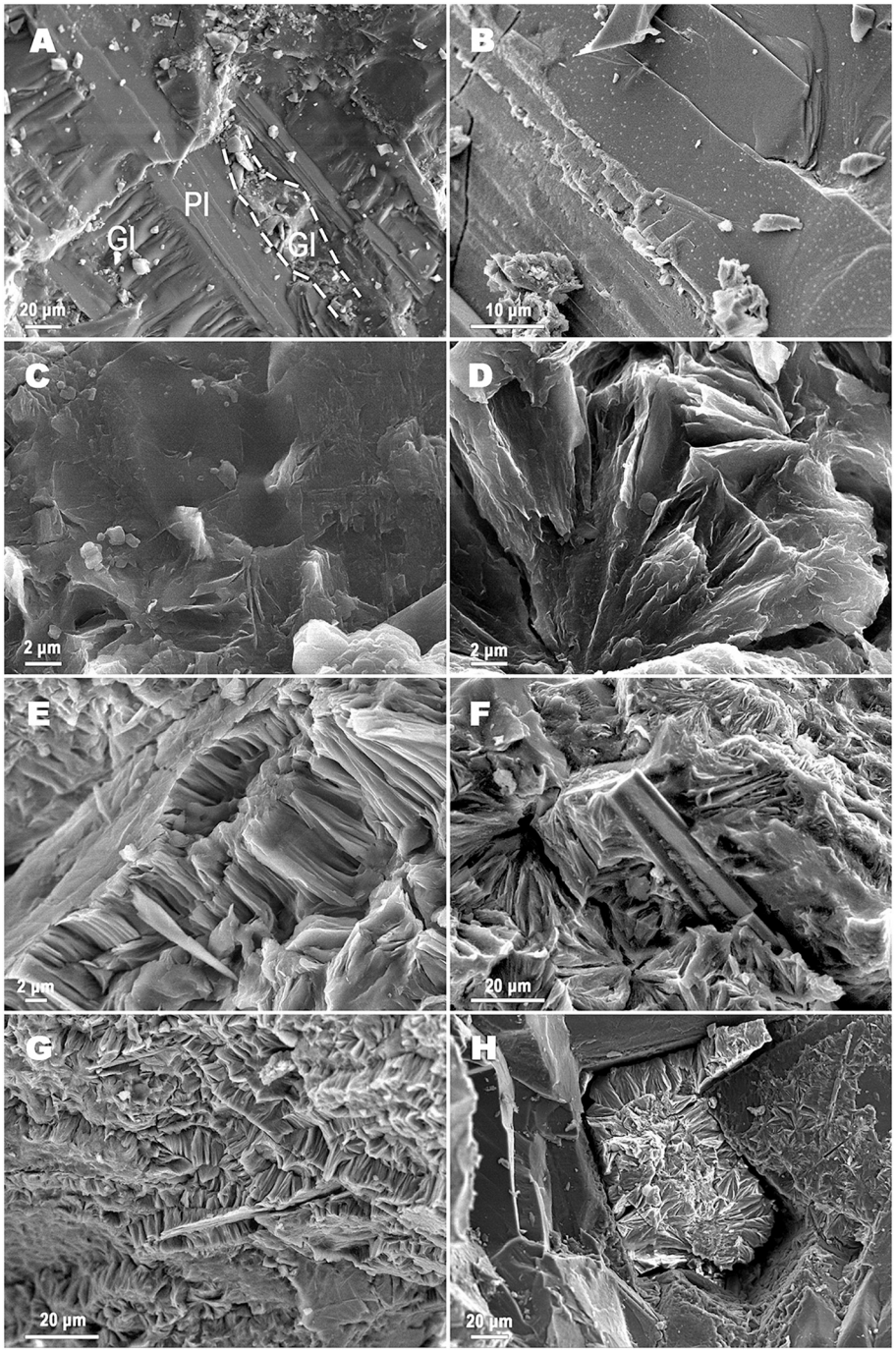

Fig. 6. Scanning electron microscopy (SEM) images that illustrate the glass to palagonite evolution. A: Unaltered glass. Dotted line indicates the limit between the glass and plagioclase. B: Unaltered glass. Apatite crystals emerge from the glass. C: Unaltered glass. Radially distributed cracks appear (see arrow). D: Radially distributed sheets. E: Layers of parallel sheets of palagonite. F and G: Representative images of palagonite. The glass has completely transformed into a mass of laminar particles. Sometimes apatite crystals are included in the palagonite. H: Palagonite surrounded of plagioclase crystals; the palagonite (smectite) swelling and shrinking effect is evident. Ap: Apatite, Gl: Glass, and Pl: Plagioclase. Mineral name abbreviations after Whitney and Evans (2010).

secondary mineral assemblages. Indeed, the following secondary assemblages formed by their alteration depend on the local physico-chemical conditions imposed by climate, water circulation, topography, or amount of microfractures that vary according to the local geological situation (Velde and Meunier, 2008).

The crystals of clinopyroxene, although fresher than those of plagioclase, are also crossed by many fractures, and they are altered at their edges. When clinopyroxenes are observed by SEM, they show deeply etched cleavage planes (Fig. 7) that are more evident when the degree of alteration is higher. As the alteration progresses, the cleavage planes become deeper, as shown in Fig. 7E, until the complete obliteration of the crystal. A structural control and topotactic and isovolumetrical mechanism occurs while chemical changes occur (Basham, 1974; Eggleton, 1975; Eggleton and Boland, 1982; Banfield and Barker, 1994), although Giorgetti et al. (2009) did not observe a topotactic relation when saponite was identified as a result of the low-temperature alteration of clinopyroxene. Banfield et al. (1995) also affirmed 'The reaction was inferred to be a diffusion-controlled, solid-state process, involving only partial depolymerisation of the amphibole structure and with no intermediate amorphous-type material'.

Parallel to the progress of alteration, the glass alters and transforms into palagonite, which is abundant in most studied samples, although in different proportions. According to Giorgetti et al. (2009), the glass-to-smectite transition can be viewed as a kinetically controlled reaction progress sequence. At the intermediate state of alteration, unaltered glass does not remain in the samples. Palagonite appears to surround the plagioclase crystals and corrodes their edges (Fig. 3E-F, and Fig. 8). It grows between and over the plagioclase crystals, moreover it clearly

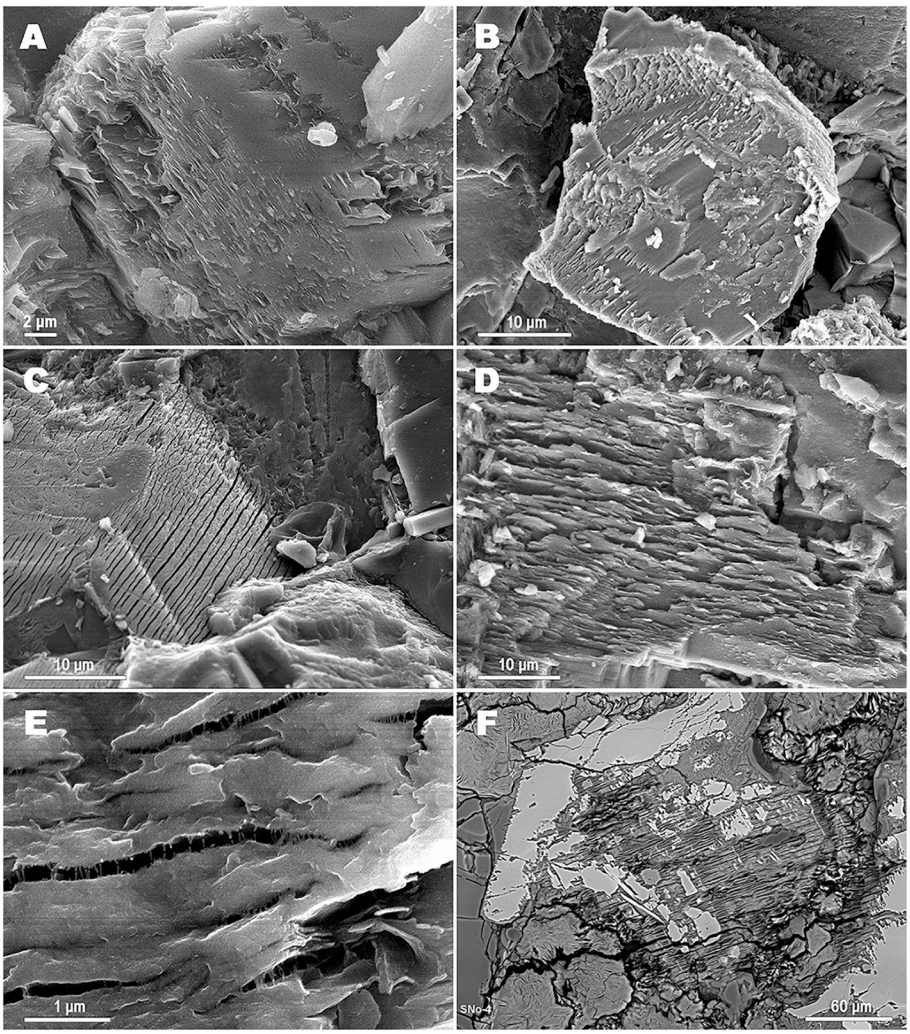

Fig. 7. Clinopyroxene (augite) images. A to E: Scanning electron microscopy (SEM) images. F: Backscattered electron (BSE) SEM image. Note the deep alteration shown by the cleavage planes.

penetrates and can be confused with the filling of the fissures of plagioclase (Fig. 8F). Fig. 6 illustrates the stages of transformation of glass to palagonite. The distributed radial cracks in the glass (Fig. 6C) transform in radially distributed sheets (Fig. 6D). Other times, they grow parallel given place to the layers of parallel sheets (Fig. 6E). Prismatic apatite crystals that appear frequently in the glass remain unaltered in the palagonite (Fig. 6F). Glass alteration sequences and the appearance of 'flake–leaf–needle morphologies' have been described in studies of experimental alteration of volcanic glass (Fiore et al., 1999; De la Fuente et al., 2000).

Based on mineralogical studies, most authors agree (Eggleton and Keller, 1982; Staudigel and Hart, 1983; Jercinovic et al., 1990; Daux et al., 1994; Stroncik and Schmincke, 2001) that palagonite is composed of a variety of smectites and very minor amounts, if any, of zeolites and oxides. The XRD patterns obtained from the raw samples and from the oriented aggregates confirm that the minerals of the alteration are smectites. The XRD patterns of raw samples in the early stage of alteration are similar to those of the intermediate stage; the only difference is the appearance of the smectite peak at low angles (Fig. 9A and B), which indicates that glass has evolved to smectite.

The SEM images (Fig. 6) indicate that the palagonitisation process is mainly isovolumetric, which agrees with the results obtained by Stroncik and Schmincke (2001) and references therein. Stroncik and Schmincke (2001, 2002) studied the evolution of palagonite and affirmed that 'a thermodynamically unstable phase undergoes a sequence of irreversible reactions over time to form progressively more stable phases. It is a continuous process of glass dissolution. The process of palagonitisation is accompanied by extensive mobilisation of all elements involved in the alteration process, resulting in the depletion or enrichment of certain elements. They also affirmed that palagonite formation and its evolution can be subdivided into two different reaction stages with changing element mobilities. The first stage is characterised by congruent dissolution of glass and contemporaneous precipitation of 'fresh', gel-like, amorphous, optically isotropic (under optical microscopy), and mainly yellowish palagonite. The second stage is an aging process during which the thermodynamically unstable palagonite reacts with the surrounding fluid and crystallises to smectite. Both processes are triggered by the mobility of chemical elements. The chemical distribution of elements in the studied samples revealed by the EDX maps (Fig. 10) agrees with that obtained by the microprobe (Table 1). Enrichment in Mg and Fe and logical impoverishment in Al, Na, and K in the palagonitic area are marked by the different grey tones in the backscattered image and also evidenced in the related maps of Mg, Fe, Al, and Na distribution. Moreover, the enrichment in K at the plagioclase edges is evident in the images.

The alteration is favoured by the fracture network; the samples are crossed by numerous nano and micro-cracks, and veins of different sizes and characteristics. Plagioclase and pyroxene phenocrysts are crossed by several small cracks that are more evident in the larger ones. The cracks are filled by smectites, which increase according to the degree of

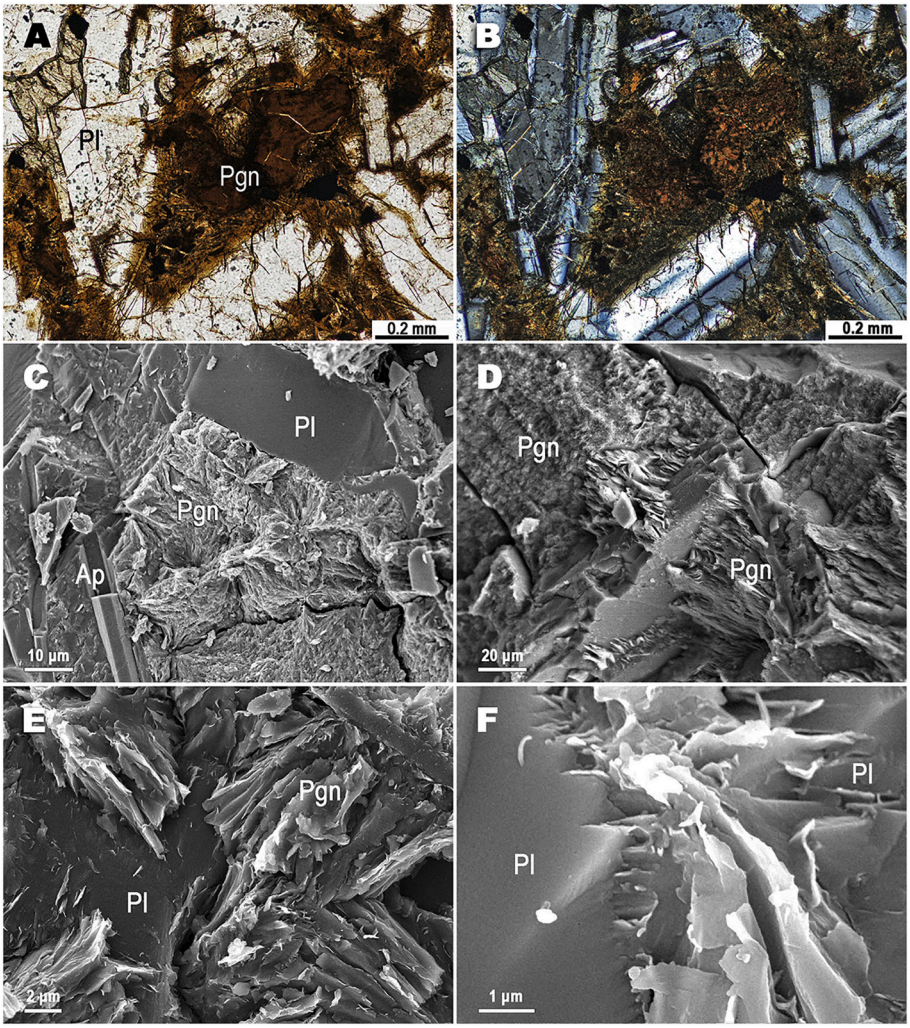

Fig. 8. A-B: Optical microscope images. C-F: Scanning electron microscopy (SEM) images. The images illustrate that the palagonite grows among and over the plagioclase crystals, wrapping them. In addition, it penetrates into the fissures. F: Smectite flakes growing at the contact between two plagioclase crystals. A: Apatite, Pl: Plagioclase, Pgn: Palagonite. Mineral name abbreviations after Whitney and Evans (2010).

alteration of the volcanic rock. Additionally, larger veins are also present (millimetre wide and centimetres long) also filled by smectites crossing the rock (Fig. 3E-H, and Fig. 11A-B) (Table 1).

6. Advanced state of alteration

In the most advanced alteration state, all the crystals and the glass are deeply affected. The overall features of the rock are clearly different from those in the earliest stages. Myriads of crystals are deeply and partially transformed mainly to smectites and the porosity of the rock increases in a process that conserves the volume. Smectite appears to be the end alteration product of both the major minerals (olivine, plagioclase, and pyroxenes) as well as the glass. The increase in the amount of smectite in the rock leads to an increase in the intensity of the characteristic 001 reflection at low angles in the XRD patterns (Fig. 9C). The smectites in the Miraflores Basalts are rich in high-charge Fe-rich beidellites (Suárez et al., 2021) and the 060 reflection appears at very high d-spacing a, 0.154 nm (Fig. 9C) which implies a content in Fe in the unit cell of ~2.1 atoms according to Heuser et al. (2013).

As the degree of alteration increases, the surface of plagioclase covered by flakes increases (Fig. 5G, H); moreover, each primary crystal is internally altered (Fig. 3G-H), as well as altered on its edges by smectite growth until it is completely transformed. At more advanced alteration stages, all the glass has completely transformed into a mass of laminar particles, frequently with a radial texture (Fig. 6F, G).

Cracks through plagioclase or pyroxene crystals greatly increase in number in the more altered areas of the Miraflores Basalt, and are dense throughout the rock in the samples from Sosa Hill Quarry, where the rock is crossed by numerous micro-cracks and veins of different sizes and characteristics. Additionally, larger veins are also present (millimetre wide and centimetres long) and are filled mainly by smectites that cross the rock; the veins sometimes are also filled with calcite and quartz (chalcedony) (Fig. 11C-F). In general, it is possible to affirm that the cracks/veins/fractures are connected and form a dense network. In addition, during this alteration process, new clay minerals are formed and new and old ones swell and shrink (Fig. 6H), which produces very high pressures and breaks the rock. The rock is altered in a continuous process, which depends on several factors such as the composition and texture of the rock, alteration agents, and exposure time. This process is gradual and self-accelerating; the more weathered the rock, the faster its alteration.

If the alteration is extreme, several of the largest veins can also be filled with different minerals, forming successive cements. Fig. 11E shows the details of a vein filled by two types of cement: i) fibrous cement surrounding newly formed grains of carbonate on the outside of the vein; and ii) mosaic cement of chalcedony in the inner part of the vein. It is possible to observe successive generations of cement in both the fibrous cement (pore-lining and pore-filling) and mosaic cement,

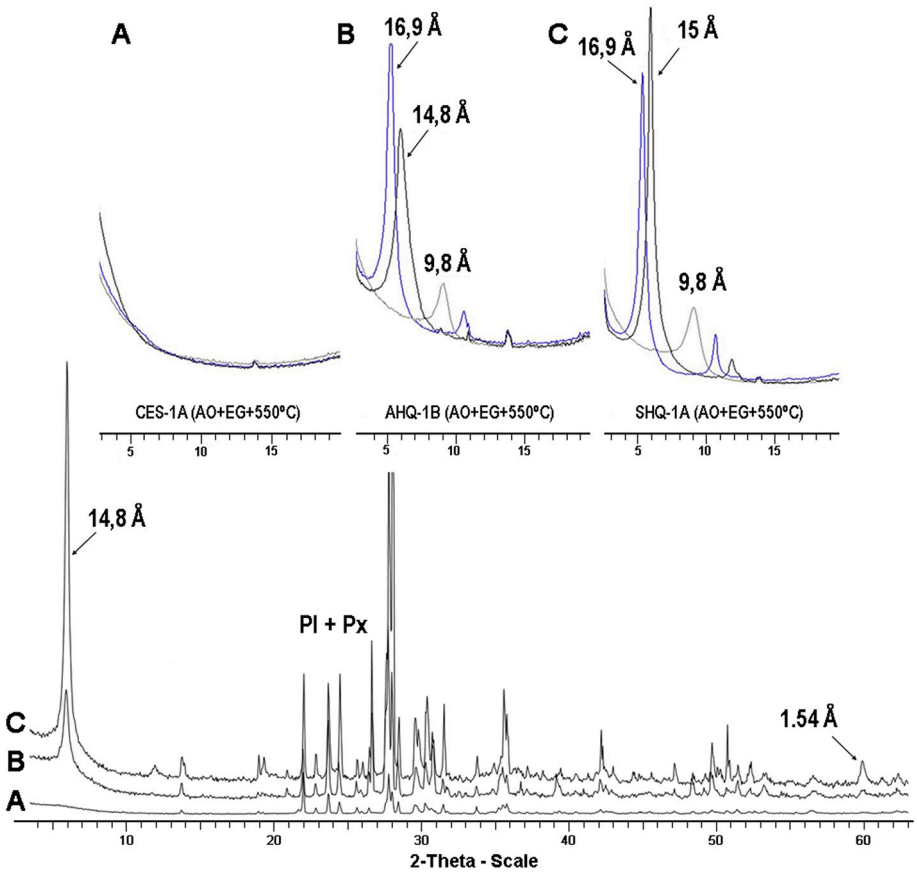

Fig. 9. XRD patterns of representative samples of A) early stage of alteration. Sample CES-1A. B) intermediate stage of alteration. Sample AHQ-1A. C) advanced stage of alteration. Sample SHQ-1A. AO: oriented aggregate (black curves), EG: oriented aggregate solvated with etylen-glycol (blue curves), 550°: oriented aggregate heated at 550° 2 h (grey curve), Pl: plagioclases, Px: pyroxenes, Sm: smectites. Mineral name abbreviations after Whitney and Evans (2010). (For interpretation of the references to colour in this figure legend, the reader is referred to the web version of this article.)

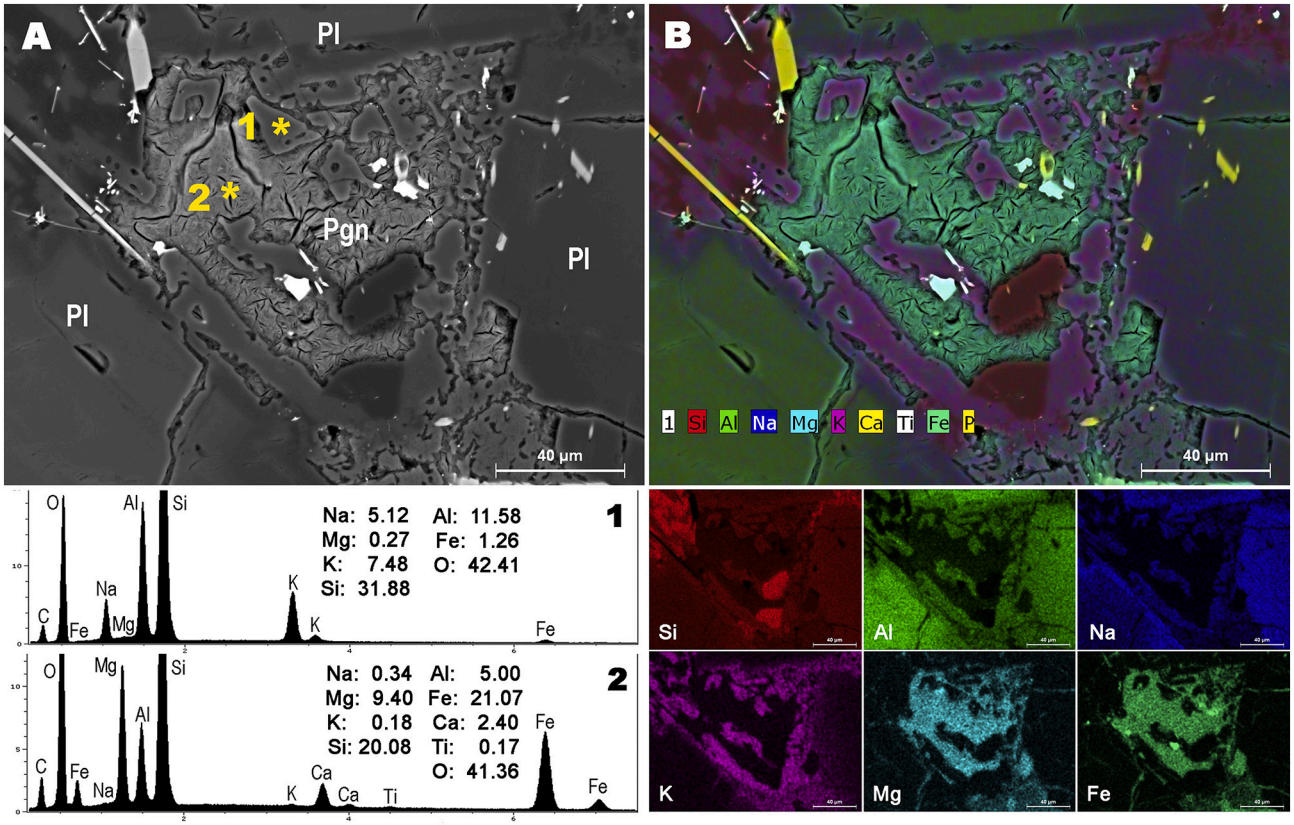

Fig. 10. A: Backscattered electron scanning electron microscopy (SEM) image. 1 and 2 graphics show the chemical composition of points 1 and 2 indicated in A. B: Coloured EDX-maps showing the chemical elemental distribution. 1: EDX glass analysis and 2: EDX Palagonite analysis. Pl: Plagioclase, Pgn: Palagonite, Mineral name abbreviations after Whitney and Evans (2010).

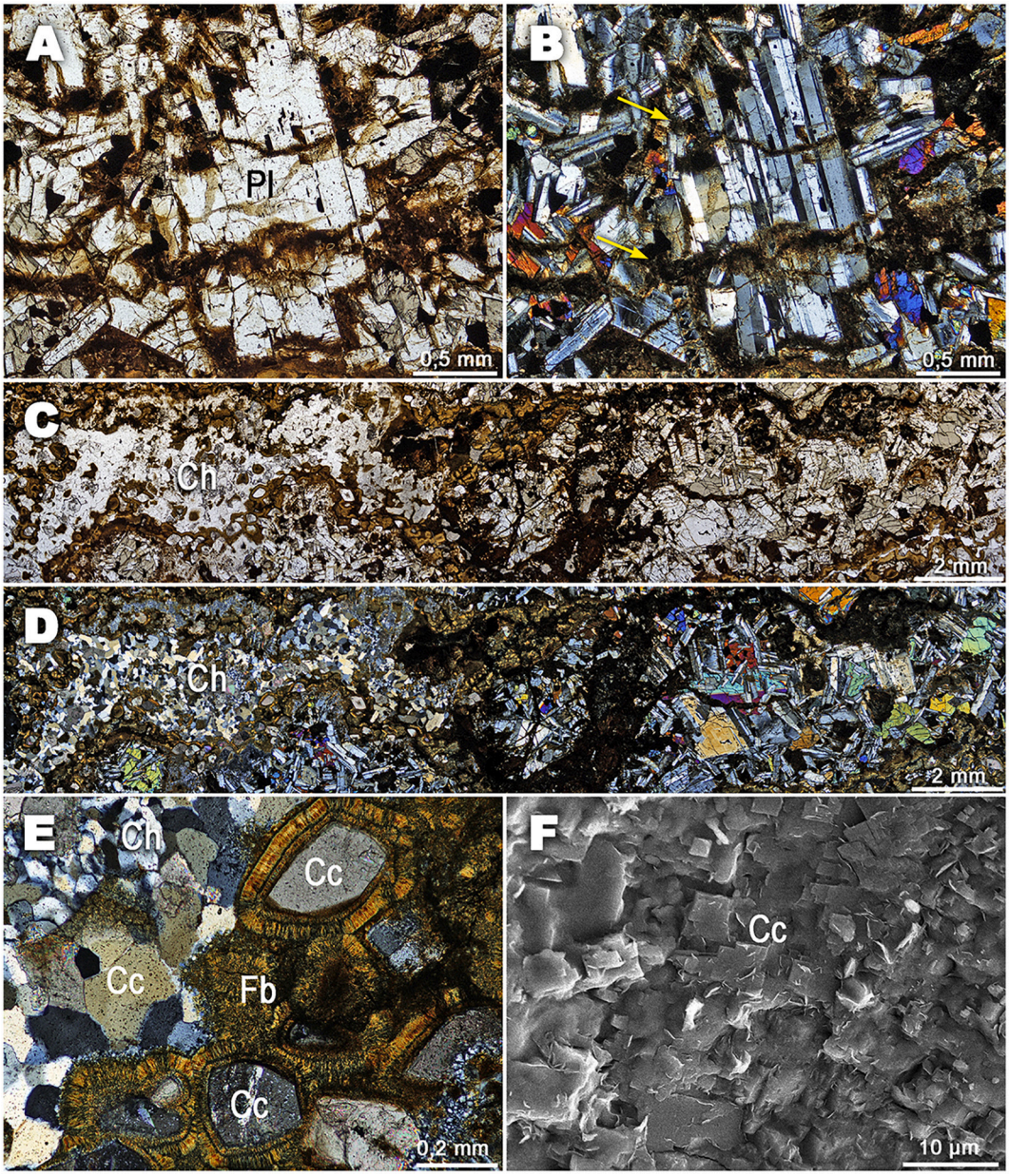

Fig. 11. A-D: Transmitted light images. B-C: Plane polarized transmitted light images. A-B: Cracks through the plagioclase crystals filled by smectite (yellow arrows). C-D: Millimetre wide and centimetres long veins filled by chalcedony. E: Large vein filled by two successive types of cement (i) fibrous cement surrounding newly formed grains of carbonate on the outside of the vein; and (ii) mosaic cement of chalcedony inside the vein. F: SEM image. Crystals of calcitic cement (sparite). Cc: Calcite, Ch: Chalcedony, Fb: Fibrous cement, and Pl: Plagioclase. Mineral name abbreviations after Whitney and Evans (2010).

which clearly indicates that the Miraflores Basalt have been subjected to successive alteration.

7. Final remarks

Evidence of the alteration processes and its development that causes basaltic rock transformation was readily obtained from OM, SEM, and EMP images. The process is clearly evidenced in Miraflores Basalt as rock samples from diverse quarries show a spatial gradation in their degree of alteration. The Cerro Escobar samples have features consistent with unaltered or weakly altered rock in both the OM and SEM images. The SEM images show that their components are strongly fused; consequently, it is difficult to differentiate the minerals from the glass. In contrast, the samples from Sosa Hill Quarry have the appearance of highly altered rock, their components are extremely altered, and their surfaces are coated by a dense mass of corrugated flakes, a product of their alteration. In addition, the glass in these samples is completely transformed to palagonite, which surrounds all the crystals. Glass only appears in the fresh volcanic rocks because it is altered during early alteration stages. Glass was only found in the relatively fresher Miraflores Basalt rocks (Cerro Escobar samples). In the other Miraflores rocks, Basalt is usually completely altered (devitrified) and transformed to palagonite.

While cracks and veins are scarce in the samples from Cerro Escobar, they greatly increase in the Pacific Site Basalt and are found as a dense framework in the samples from Sosa Hill Quarry. Moreover, while the plagioclase and pyroxenes crystals from Cerro Escobar are clean, those from other Miraflores Basalts show evident signs of alteration including corrosion at the edges of the faces and in the interior of the crystals; both types of corrosion are more evident in larger crystals. Alteration is

usually favoured by fractures, zoning, and inclusions. In addition, the progressive alteration of ferromagnesian minerals is clear.

Declaration of Competing Interest

The authors declare that they have no known competing financial interests or personal relationships that could have appeared to influence the work reported in this paper.

Acknowledgements

We want to thank GUPC for allowing us to use their facilities to conduct this work. This work has been partially funded by Spanish Ministerio de Ciencia e Innovación (grant number PID-2019-106504RB-100).

References

Banfield, J.F., Barker, W.W., 1994. Direct observation of reactant-product interfaces formed in natural weathering of exsolved defective amphibole to smectite: evidence for episodic, isovolumetric reactions involving structural inheritance. Geoch. Cosmoch. Acta. 58, 1419–1429.
Banfield, J.F., Veblen, D.R., Jones, B.F., 1990. Transmission electron microscopy of subsolidus oxidation and weathering of olivine. Contrib. Mineral. Petrol. 106, 110–123.
Banfield, J.F., Ferruzzi, G.G., Casey, W.H., Westrich, H.R., 1995. HRTEM study comparing naturally and experimentally weathered pyroxenoids. Geoch. Cosmoch. Acta. 59, 1931.
Basham, I.R., 1974. Mineralogical changes associated with deep weathering of gabbro in Aberdeenshire. Clay Miner. 10, 189–202.
Bhattacharyya, T., Pal, D.K., Deshpande, S.B., 1992. Genesis and transformation of minerals in the formation of red (Alfisols) and black (Inceptisols and Vertisols) soils on Deccan basalt in western Ghats, India. J. Soil Sci. 44, 159–171.
Böhlke, J.K., Honnorez, J., Honnorez-Guerstein, M., 1980. Alteration of Basalts from Site 396B, DSDP: Petrographic and Mineralogic Studies. Contrib. Mineral. Petrol. 73, 341–364.
Böhlke, J.K., Honnorez, J., Honnorez-Guerstein, B.M., Muehlenbachs, K., Petersen, N., 1981. Heterogeneous alteration of the upper ocean crust: correlation of rock chemistry, magnetic properties, and O isotope ratios with alteration patterns in basalts from site 396B. DSDP. Journ. Geophys. Research 86 (B9), 7935–7950.
Brigatti, M.F., 1983. Relationships between composition and structure in Fe-rich smectites. Clay Miner. 18, 177–186.
Chadwick, O.A., Gavenda, R.T., Kelly, E.F., Ziegler, K., Olson, C.G., Elliott, W.C., Hendricks, D.M., 2003. The impact of climate on the biogeochemical functioning of volcanic soils. Chem. Geol. 202, 195–223.
Christidis, G.E., 2001. Formation and growth of smectites in bentonites: a case study from Kimolos Island, Aegean, Greece. Clays Clay Miner. 49, 204–215.
Christidis, G.E., 2006. Genesis and compositional heterogeneity of smectites. Part III: Alteration of basic pyroclastic rocks. A case study from the Troodos Ophiolite complex. Cyprus. Am. Mineral. 91, 685–701.
Christidis, G.E., Hu, W.D., 2009. Geological Aspects and Genesis of Bentonites. Elements 5, 93–98.
Churchman, G.J., Lowe, D.J., 2012. Alteration, formation, and occurrence of minerals in soils. In: Huang, P.M., Li, Y., Sumner, M.E. (Eds.), Handbook of Soil Sciences, Properties and Processes, 2nd ed., vol. 1. CRC Press (Taylor & Francis), Boca Raton, FL, pp. 20.1–20.72.
Colman, S.M., 1982. Chemical weathering of basalts and andesites: Evidence from weathering rinds. In: Geological Survey Professional Paper 1246. US Department of the Interior, United States Government Printing Office, Washington.
Craigh, D.C., Loughnan, F.C., 1964. Chemical and mineralogical transformations accompanying the weathering of basic volcanic rocks from New South Wales: Australian. J. Soil Res. 2, 218–234.
Cuadros, J., Dekov, V.M., Arroyo, X., Nieto, F., 2011. Smectite formation in submarine hydrothermal sediments: Samples from the HMS Challenger expedition (1872–1876). Clay Clay Miner. 59, 147–164.
Daux, V., Crovisier, J.L., Hemond, C., Petit, J.C., 1994. Geochemical evolution of basaltic rocks subjected to weathering: fate of the major elements, rare earth elements, and thorium. Geochim. Cosmochim. Acta 58, 4941–4954.
De la Fuente, S., Cuadros, J., Fiore, S., Linares, J., 2000. Electron microscopy study of volcanic tuff alteration to illite-smectite under hydrothermal conditions. Clay Clay Miner. 48 (3), 339–350.
Decarreau, A., Colin, F., Herbillon, A., Manceau, A., Nahon, D., Paquet, H., Trauth-Badeaud, D., Trescases, J.J., 1987. Domain segregation in Ni-Fe-Mg-smectites. Clay Clay Miner. 35, 1–10.
Delvaux, B., Herbillon, A.J., 1995. Pathways of mixed-layer kaolin–smectite formation in soils. In: Churchman, G.J., Fitzpatrick, R.W., Eggleton, R.A. (Eds.), Clays Controlling the Environment: Proceedings of the 10th International Clay Conference. Adelaide, Australia, pp. 457–461.
Delvigne, J., Bisdom, E.B.A., Sleeman, J., Stoops, G., 1979. Olivines, their pseudomorphs and secondary products. Pedologie 29, 247–309.
Eggleton, R.A., 1975. Nontronite topotaxial after hedenbergite. Am. Mineral. 60, 1063–1068.
Eggleton, R.A., 1984. Formation of iddingsite rims on olivine: a transmission electron microscope study. Clay Clay Miner. 32, 1–11.
Eggleton, R.A., Boland, J.N., 1982. Weathering of enstatite to talc through a sequence of transitional phases. Clay Clay Miner. 30, 1120.
Eggleton, R.A., Keller, J., 1982. The palagonitization of limburgite glass – a TEM study. Neues Jahrb Miner. 7, 321–336.
Eggleton, R.A., Foudoulis, C., Varkevisser, D., 1987. Weathering of basalt: changes in rock chemistry and mineralogy. Clay Clay Miner. 35 (3), 161–169.
Farris, D.W., Cardona, A., Montes, C., Foster, D., Jaramillo, C., 2017. Magmatic evolution of Panama Canal volcanic rocks: a record of arc processes and tectonic change. PLoS One 12 (5), e0176010. https://doi.org/10.1371/journal.pone.0176010.
Fiore, S., Huertas, J., Tazaki, K., Huertas, F., Linares, J., 1999. A low temperature experimental alteration of a rhyolitic obsidian. Eur. J. Mineral. 11, 455–469.
Fontaine, F., Christidis, G.E., Yans, J., Hollanders, S., Hoffman, A., Fagel, N., 2020. Characterization and origin of two Fe-rich bentonites from Westerwald (Germany). Appl. Clay Sci. 187 (art. 105444).
Fookes, P.G., Gourley, C.S., Ohikere, C., 1988. Rock weathering in engineering time. Q. J. Eng. Geol. 21, 33–57.
Furnes, H., 1980. Chemical changes during palagonitization of an alkaline olivine basa. ltic hyaloclastite, Santa Maria, Azores. Neues Jahrb. Miner. Abh. 138, 14–30.
Furnes, H., 1984. Chemical-changes during progressive subaerial palagonitization of a subglacial olivine tholeiite hyaloclastite – a microprobe study. Chem. Geol. 43, 271–285.
García-Romero, E., Vegas, J., Baldonedo, J.L., Marfil, R., 2005. Clay minerals as alteration products in basaltic volcaniclastic deposits of La Palma (Canary Islands, Spain). Sediment. Geol. 174, 237–253.
García-Romero, E., Manchado, E.M., Suárez, M., García-Rivas, J., 2019. Spanish bentonites: a review and new data on their geology, mineralogy, and crystal chemistry. Minerals 9, 696.
Gaudin, A., Dehouck, E., Grauby, O., Mangold, N., 2018. Formation of clay minerals on Mars: Insights from long-term experimental weathering of olivine. Icarus 311, 210–223.
Gillis, K.M., Robinson, P.T., 1990. Patterns and processes of alteration in the lavas and dykes of the Troodos Ophiolite, Cyprus. J. Geophys. Res. 95, 21,523–21,548.
Giorgetti, G., Monecke, T., Kleeberg, R., Hannington, M.D., 2009. Low-temperature hydrothermal alteration of trachybasalt at conical seamount, Papua New Guinea: Formation of smectite and metastable precursor phases. Clays Clay Miner. 57, 725–741.
Heuser, M., Andrieux, P., Petit, S., Stanjek, H., 2013. Iron-bearing smectites: a revised relationship between structural Fe, b cell edge lengths and refractive indices. Clay Miner. 48, 97–103.
Huertas, F.J., Cuadros, J., Huertas, F., Linares, J., 2000. Experimental study of the hydrothermal formation of smectite in the beidellite-saponite series. Am. J. Sci. 300, 504–527.
Jercinovic, M.J., Keil, K., Smith, M.R., Schmitt, R.A., 1990. Alteration of basaltic glasses from north-Central British Columbia, Canada. Geochim. Cosmochim. Acta. 54, 2679–2696.
Kadir, S., Külah, T., Önalgil, N., Erkoyun, H., Elliott, W.C., 2017. Mineralogy, geochemistry, and genesis of bentonites in miocene volcanic-sedimentary units of the Ankara-Çankiri Basin, Central Anatolia, Turkey. Clays Clay Miner. 65, 64–91.
Köster, H.M., Ehrlicher, U., Gilg, H.A., Jordan, R., Murad, E., Onnich, K., 1999. Mineralogical and chemical characteristics of five nontronites and Fe-rich smectites. Clay Miner. 34, 579–599.
Lacoviello, F., Giorgetti, G., Nieto, F., Memmi, I.T., 2012. Evolution with depth from detrital to authigenic smectites in sediments from AND-2A drill core (McMurdo Sound, Antarctica). Clay Miner. 47, 481–498.
Loughnan, F.C., 1969. Chemical Weathering of Silicate Minerals. Elsevier, New York, 154 pp.
Manuella, F.C., Carbone, S., Barreca, G., 2012. Origin of Saponite-Rich Clays in a Fossil Serpentinite-Hosted Hydrothermal System in the Crustal Basement of the Hyblean Plateau (Sicily, Italy). Clay Clay Miner. 60, 18–31.
Meunier, A., Sardini, P., Robinet, J.C., Pret, D., 2007. The petrography of weathering processes: Facts and outlooks. Clay Miner. 42 (4), 415–435.
Nesbitt, H.W., Wilson, R.E., 1992. Recent chemical weathering of basalts. Am. J. Sci. 292, 740–777.
Peacock, M.A., Fuller, R.E., 1928. Chlorophaeite, sideromelane and palagonite from the Columbia River Plateau. Am. Mineral. 13, 360–383.
Rasmussen, C., Dahlgren, R.A., Southard, R.J., 2010. Basalt weathering and pedogenesis across an environmental gradient in the southern Cascade Range, California, USA. Geoderma 154 (3–4), 473–485.
Righi, D., Terribile, F., Petit, S., 1999. Pedogenic formation of kaolinite-smectite mixed layers in a soil toposequence developed from basaltic parent material in Sardinia (Italy). Clays Clay Miner. vol. 47 (4), 505–514.
Smith, K.L., Milnes, A.R., Eggleton, R.A., 1987. Weathering of Basalt: Formation of iddingsite. Clay Clay Miner. 35 (6), 418–428.
Środoń, J., Kuzmenkova, O., Stanek, J.J., Petit, S., Beaufort, D., Albert Gilg, H., Liivamägi, S., Goryl, M., Marynowski, L., Szczerba, M., 2019. Hydrothermal alteration of the Ediacaran Volyn-Brest volcanics on the western margin of the east European Craton. Precambrian Res. 325, 217–235.
Staudigel, H., Hart, S.R., 1983. Alteration of basaltic glass: mechanisms and significance for the oceanic crust-sea water budget. Geochim. Cosmochim. Acta 47, 337–350.
Stefansson, A., Gislason, S.R., 2001. Chemical weathering of basalts, southwest Iceland: effect of rock crystallinity and secondary minerals on chemical fluxes to the ocean. Am. J. Sci. 301, 513–556.

Stewart, R.H., Stewart, J.L., Wooding, W.P., 1980. Geologic map of the Panama Canal and vicinity, Republic of Panama. United States Geological Survey (USGS). In: Miscellaneous investigations series map I-1232. https://doi.org/10.3133/i1232.
Stroncik, N.A., Schmincke, H.U., 2001. Evolution of palagonite: Crystallization chemical changes, and element budget. Geochemistry Geophysics, Geosystems 2 (Paper number 2000GC000102).
Stroncik, N.A., Schmincke, H.U., 2002a. Palagonite – a review. Int J. Earth. Sci. (Geol Rundsch). 91, 680–697.
Stroncik, N.A., Schmincke, H.U., 2002b. Palagonite – a review. Int. J. Earth. Sci. (Geol Rundsch) 9, 680–697.
Suárez, M., García Romero, E., Baz, A., Pérez, R., 2021. Smectites: the key to the cost overruns in the construction of the third set of locks of the Panama Canal. Engineer. Geol. https://doi.org/10.1016/j.enggeo.2021.106036.
Thanachit, S., Suddhiprakarn, A., Kheoruenromne, I., Gilkes, R.J., 2006. The geochemistry of soils on a catena on basalt at Khon Buri, Northeast Thailand. Geoderma 135, 81–96.
Ugolini, F.C., 1974. Hydrothermal origin of the clays from the upper slopes of Mauna Kea, Hawaii. Clays Clay Miner. 22, 189–194.
Velde, B., Meunier, A., 2008. The Origin of Clay Minerals in Soils and Weathered Rocks. Springer-Verlag, Berlin Heidelberg (407 pp).
Vingiani, S., Terribile, F., Meunier, A., Petit, S., 2010. Weathering of basaltic pebbles in a red soil from Sardinia: a microsite approach for the identification of secondary mineral phases. Catena 83 (2–3), 96–106.
Von Waltershausen, W.S., 1845. Über die submarinen Ausbrüche in der tertiären Formation des Val di Noto im Vergleich mit verwandten Erscheinungen am Ätna. Gött Stud 1, 371–431.
Whitney, D.L., Evans, B.W., 2010. Abbreviations for names of rock-forming minerals. Am. Mineral. 95, 185–187.
Wilson, M.J., 2004. Weathering of the primary rock-forming minerals: processes, products and rates. Clay Miner. 39, 233–266.
Yesavage, T., Thompson, A., Hausrath, E.M., Brantley, S.L., 2015. Basalt weathering in an Arctic Mars-analog site. Icarus 254 (2015), 219–232.
Zhou, Z.H., Fyfe, W.S., Tazaki, K., Vandergaast, S.J., 1992. The structural characteristics of palagonite from DSDP Site-335. Can. Mineral. 30, 75–81.